JASA Express Letters

JANUARY 10 2024

Performance of three hydrophone flow shields in a tidal channel

Emma Cotter ; James McVey ; Linnea Weicht ; Joseph Haxel

JASA Express Lett. 4, 016001 (2024)
https://doi.org/10.1121/10.0024333

JASA EXPRESS LETTERS ARTICLE asa.scitation.org/journal/jel

Performance of three hydrophone flow shields in a tidal channel

Emma Cotter,[a] James McVey, Linnea Weicht, and Joseph Haxel
Coastal Sciences Division, Pacific Northwest National Laboratory, Sequim, Washington 98382, USA
emma.cotter@pnnl.gov, james.mcvey@pnnl.gov, linnea.weicht@pnnl.gov, joseph.haxel@pnnl.gov

Abstract: Pseudosound caused by turbulent pressure fluctuations in fluid flow past a hydrophone, referred to as flow noise, can mask propagating sounds of interest. Flow shields can mitigate flow noise by reducing non-acoustic pressure fluctuations sensed by a hydrophone. We evaluate the performance of three hydrophone flow shields (two nylon fabrics and an oil-filled enclosure) in a tidal channel with peak current speed of 1.3 m s^{-1}. All three flow shields reduced flow noise without attenuating propagating sound below 20 kHz. The oil-filled enclosure performed best, reducing flow noise by over 30 dB at frequencies below 40 Hz.

[Editor: Gopu R. Potty] https://doi.org/10.1121/10.0024333

Received: 29 September 2023 **Accepted:** 22 December 2023 **Published Online:** 10 January 2024

1. Introduction

When water moves over a hydrophone, it can cause low-frequency pseudosound often referred to as flow noise.[1,2] Flow noise results from pressure fluctuations associated with freestream turbulence advected over the sensor and the turbulent wake produced by the sensor itself. In some cases, flow noise can be of sufficient magnitude to mask propagating sounds of interest.[3] The effect of flow noise increases in amplitude with current speed and turbulence intensity, which makes it a persistent challenge for acoustic monitoring in environments with strong flows, such as tidal channels or rivers. For example, Bassett *et al.*[4] measured flow noise in two tidal channels and found that flow noise effects exceeded ambient levels by over 50 dB at the lowest frequencies measured (20 Hz) and impacted measurements at frequencies up to 500 Hz at peak current speeds of 3 m s^{-1}.

There are a variety of approaches to address the flow noise problem. The most straightforward is to place hydrophones in an area of quiescent water where flow noise will be minimized, although this is not feasible at many sites. Alternatively, drifting hydrophone systems can reduce the relative velocity between the water and the hydrophone, but surveys are time- and labor-intensive and cannot capture long-term temporal variability in high current environments.[5] When fixed-station recordings are preferable, flow shields that reduce the current-induced pressure fluctuations sensed by the hydrophone are an attractive approach to flow noise mitigation. However, if noise reduction by the flow shield is not well characterized, it may not be possible to determine whether recorded low-frequency sounds are attributable to flow noise or propagating sound.[6]

A number of flow shield designs have been employed at energetic sites with varying success. Thin nylon flow shields have been used in several studies, although their performance has not been quantitatively assessed.[7] Notably, at a wave energy site with significant wave orbital velocities, a thin nylon flow shield was found to be ineffective and produced a fluttering sound during peak wave conditions.[8] A flow shield made of a relatively thick nylon material (ballistic nylon) was found to suppress flow noise contamination by 10–15 dB in a tidal channel.[9] Bassett[10] evaluated a flow shield made from porous foam enclosed in a rigid plastic mesh housing and found that it reduced flow noise by over 30 dB at 20 Hz in a tidal channel. Porskamp *et al.*[11] also reported that a flow shield made of acoustic foam was effective, although flow noise reduction was not quantified.

While these studies offer some insight into useful flow shield design, few quantitative evaluations have been performed, and, to our knowledge, no side-by-side performance comparisons of various flow shield designs have been made. To address this gap, we compare the performance of three flow shield designs in a tidal channel. The results offer insight into how flow shields may significantly improve data quality for passive acoustic monitoring at high current sites.

[a]Author to whom correspondence should be addressed.

2. Methods

2.1 Instrumentation and test site

Four commercial off-the-shelf Ocean Instruments (Auckland, New Zealand) SoundTrap ST600 HF hydrophones (1.5 cm diameter) were mounted to a Sea Spider lander (Oceanscience, Carlsbad, CA) using a custom mount [Fig. 1(a)]. Three hydrophones were outfitted with flow shields, while the fourth unshielded hydrophone provided a baseline measurement. A Nortek (Rud, Norway) Vector acoustic Doppler velocimeter (ADV) was mounted in the center of the hydrophones, with the x axis of the ADV head set perpendicular to the line of sensors. The hydrophones were configured to continuously acquire data at 96 kHz recorded in 5 min WAV files. The ADV recorded data at 16 Hz and transmitted at an acoustic frequency of 6 MHz. Low-frequency calibrations were performed for all hydrophones by Ocean Networks Canada between 1 and 700 Hz. While analysis of flow noise in this work is limited to frequencies below 700 Hz, higher-frequency data are used to evaluate whether the flow shields attenuated propagating sound. High-frequency calibrations were performed for three hydrophones at Pacific Northwest National Laboratory between 50 000 and 180 000 Hz. The linear mean of the high-frequency sensitivities of these three hydrophones was assumed to be representative of the sensitivity of the fourth hydrophone, which was outfitted with the oil-filled flow shield. This assumption was deemed acceptable because the sensitivities of the three hydrophones were within 1 dB at the frequencies analyzed in this paper.

The lander was deployed in the narrow tidal channel at the entrance to Sequim Bay, WA (48.079° N, 123.043° W). The tidal channel is approximately 250 m wide with a maximum depth of 11 m and peak current speeds exceeding 2 m s^{-1}. Because the variable bathymetry of the inlet produces sharp gradients and asymmetries in the tidal currents, a previously performed acoustic Doppler current profiler (ADCP) survey[12] was used to select a deployment location that experienced relatively fast and symmetrical current speeds during ebb and flood tides. The instrumented lander was deployed from January 31 to February 6, 2023 during a spring tide. Divers oriented the lander such that the line of sensors was approximately perpendicular to the dominant flow direction (x axis of the ADV aligned with the flood tide) to minimize flow interactions between sensors. A nearby water intake pump produced continuous tones at 168 and 336 Hz, respectively.

2.2 Flow shields

The three flow shields that were evaluated are shown in Figs. 1(b)–1(d): thin nylon, thick ballistic nylon, and an oil-filled enclosure (nylon, ballistic nylon, and oil-filled). The nylon and ballistic nylon shields have the same operating principle: They retard the flow and suppress turbulence around the hydrophone. These materials were selected due to their previous application at high-energy sites. The nylon flow shield was stretched over the hydrophone cage, while a custom urethane cage was used to support the ballistic nylon shield. The fabrics were pulled taught to avoid fluttering and secured with a hose clamp. Urethane components were cast using a vacuum to avoid the formation of bubbles that could interfere with and attenuate acoustic signals.

The oil-filled enclosure has a different operating principle—it effectively increases the size of the hydrophone, which increases the length scales of turbulent fluctuations that will partially cancel out over the body of the flow shield.[4] Because the length scales of turbulent fluctuations are inversely related to their frequency, this results in a faster roll-off (steeper slope) of flow noise contamination with increasing frequency. Like the ballistic nylon shield cage, the oil enclosure was made of urethane and cast using a vacuum. The urethane had a density approximately equal to that of seawater (1020 kg m^{-3}) and a medium-soft durometer, which allowed the material to form a watertight seal while maintaining structural rigidity. The enclosure had a diameter of 7 cm (4.5 times larger than the diameter of the hydrophone) and was filled with mineral oil before being sealed with a hose clamp. A groove at the base of the shield prevented the hose clamp from slipping, and a slot cut out of the base of the shield allowed the material to be pulled tight around the hydrophone body. Acoustic attenuation in the mineral oil layer is negligible at frequencies less than 500 kHz [<0.2 dB cm^{-1} at 500 kHz (Ref. 13)]. We note that this flow shield design is similar to oil-filled transducers used in laboratories, surface ships, and submarines.[14,15]

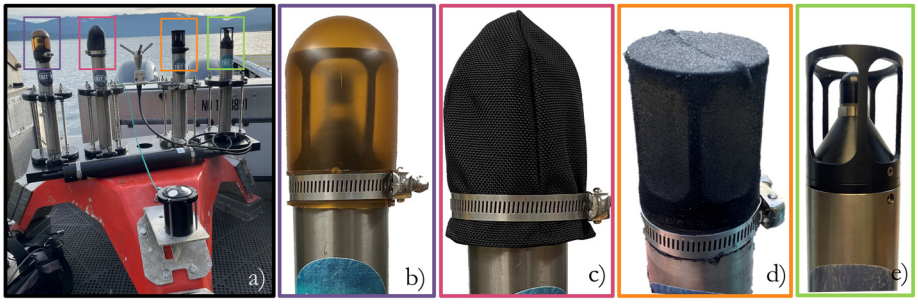

Fig. 1. (a) Instrumentation lander with hydrophones and ADV prior to deployment; (b) oil-filled flow shield; (c) ballistic nylon flow shield; (d) thin nylon flow shield; (e) unshielded hydrophone.

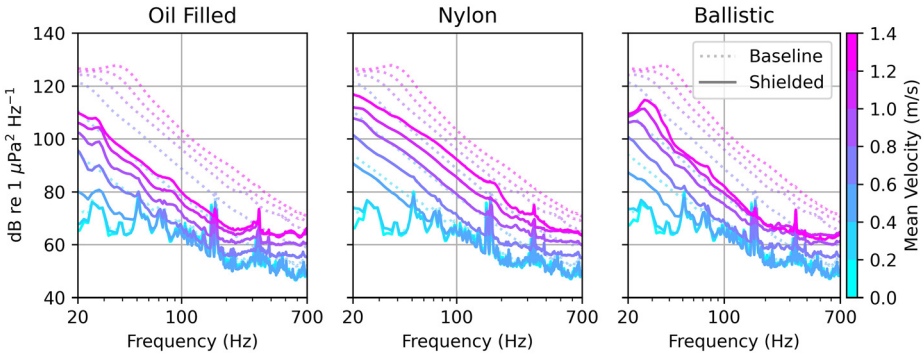

Fig. 2. Mean power spectral density in 0.2 m s^{-1} water velocity bins for the hydrophones fitted with the oil-filled, nylon, and ballistic nylon flow shields. The dashed lines indicate sound levels recorded by the unshielded hydrophone.

2.3 Data analysis

For each hydrophone, spectrum levels were calculated in 1.5 s (2^{16}-point) windows with 50% overlap. A Hamming window was used to taper each window before calculating the spectra using a direct Fourier transform, yielding a frequency resolution of 1.5 Hz. A spectrogram of each 5-min file recorded by the unshielded hydrophone was manually reviewed to identify and isolate time windows contaminated by noise from passing vessels or impulsive noise due to objects (e.g., cobblestones) impacting the lander. A windstorm on February 3, when wind gusts exceeded 15 m s^{-1}, resulted in elevated broadband sound levels[16] at the beginning of an ebb tide. These data were removed from subsequent analysis.

Acoustic spectra were averaged for each 5-min file to create a long-term spectral average. Velocity data from the ADV were processed using the Doppler Oceanography Library for Python (DOLfYN).[17] Spurious datapoints in ADV-measured velocity, termed "spikes," are caused by a number of factors, including high turbulence intensity, bubbles, organic matter, and/or Doppler phase ambiguity.[18] Data were "de-spiked" following Goring and Nikora[19] and Wahl[18] using a window size of 5000 points. Data points with correlation values lower than 70% were also removed. Removed data points were filled using cubic spline interpolation before calculating mean velocities in the same 5-min windows as the acoustic data.[19]

After averaging the acoustic and velocity data, the mean acoustic power spectral density was calculated in 0.2 m s^{-1} water velocity magnitude bins. Additionally, flow noise contamination was estimated as a function of water velocity and flow direction (ebb/flood tide) in 0.2 m s^{-1} bins by subtracting the mean power spectral density from −0.1 to 0.1 m s^{-1} (where negative values indicate ebb tide) from the mean power spectral density level in each subsequent bin.

3. Results

Figure 2 shows the mean power spectral density in 0.2 m s^{-1} current speed bins for each shielded hydrophone compared to the unshielded hydrophone, and Fig. 3 shows the flow noise contamination measured by each hydrophone as a function of water velocity during ebb and flood tides at three representative frequencies. Peaks in mean sound levels recorded by the unshielded hydrophone and the hydrophones with the oil-filled and ballistic nylon flow shields between 20 and 40 Hz may be attributed to noise on the hydrophone lander (e.g., loose recovery line or entrained debris). All three shields effectively reduced flow noise contamination. This is demonstrated clearly by the tones associated with the water intake pump:

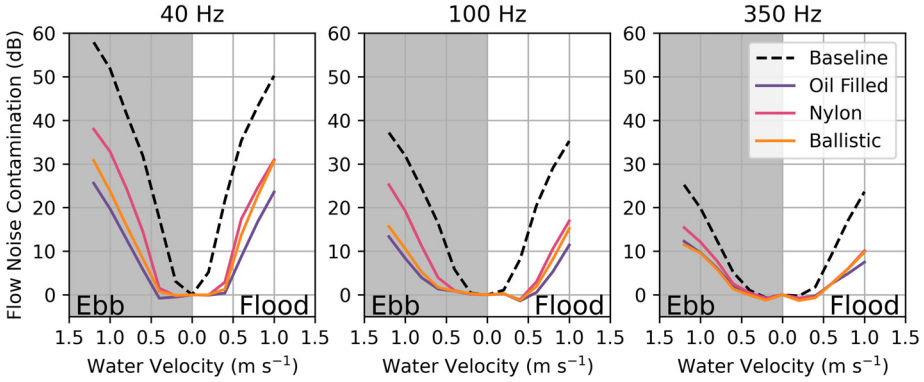

Fig. 3. Flow noise contamination recorded by each hydrophone at 40, 100, and 350 Hz on ebb and flood tides as a function of water velocity.

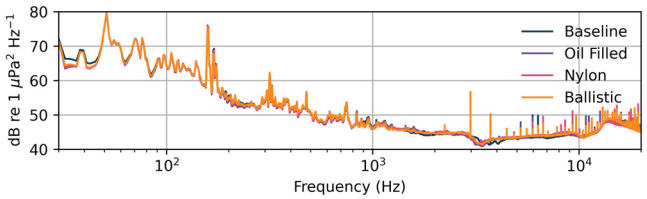

Fig. 4. Mean sound levels from 0 to 0.2 m/s flow speeds as measured by each hydrophone. Spikes above 3000 Hz can be attributed to electrical line noise in the SoundTrap hydrophones at higher frequencies.

The 336 Hz tone was not detectable by the unshielded hydrophone when flow speeds exceeded 0.8 m s^{-1} but is detectable at peak flow conditions in data from all three shielded hydrophones. At peak recorded flow velocities (1.2–1.4 m s^{-1}), baseline sound levels were elevated 59 dB above slack conditions at 40 Hz. At the same frequency and flow speeds, the oil-filled, nylon, and ballistic nylon flow shields reduced mean flow noise contamination by 31, 19, and 25 dB, respectively. The performance of the ballistic nylon flow shield approached that of the oil-filled flow shield at higher frequencies; at 100 Hz, the oil-filled, nylon, and ballistic nylon flow shields reduced mean flow noise contamination by 23, 11, and 21 dB at 100 Hz, respectively.

As evidenced in Fig. 3, both the measured flow noise contamination and the reduction in noise by the flow shields varied between ebb and flood tides. Increased flow noise contamination during flood tides may be attributed to a higher turbulence dissipation rate than ebb tides (see supplemental Fig. S1). Differences in flow shield performance between ebb and flood tides may be related to turbulence conditions or could be related to asymmetry in tidal direction if hydrophones were in the wake of other instrumentation (see supplemental Fig. S2). Notably, the nylon shield reduced flow noise by 18 dB at 100 Hz at 0.9–1.1 m s^{-1} on flood tides, but only 13 dB on ebb tides.

Figure 4 shows mean sound levels measured by all four hydrophones at slack tide (0–0.2 m s^{-1} bin). Slack tide sound levels are within 2 dB between 30 Hz and 2 kHz (Fig. 4). Above 2 kHz, electrical line noise affected measurements, but visual inspection indicates that mean sound levels are comparable between the four hydrophones between 2 and 20 kHz. This indicates that none of the flow shields significantly attenuated propagating sound at these frequencies.

Peaks were observed in the sound levels recorded by the oil-filled shielded hydrophone during strong currents at approximately 800, 2000, and 3000 Hz that were not measured by the other hydrophones. Similarly, peaks observed near 900 and 3000 Hz in the unshielded hydrophone data are not observed in data from the other hydrophones (Fig. 5). These frequencies are above the range affected by flow noise, but increases in sound levels during peak flow speeds are observed due to sediment mobilization and entrained air at the water surface. These signals are associated with a "thumping" sound in the audio recordings and may be the result of kelp or other plant matter caught on the hydrophones flapping during tidal exchanges. The fabric flow shields protected the hydrophone element from direct contact with plant matter, while plant matter contact with the exterior of the oil-filled flow shield or unshielded hydrophone would be sensed.

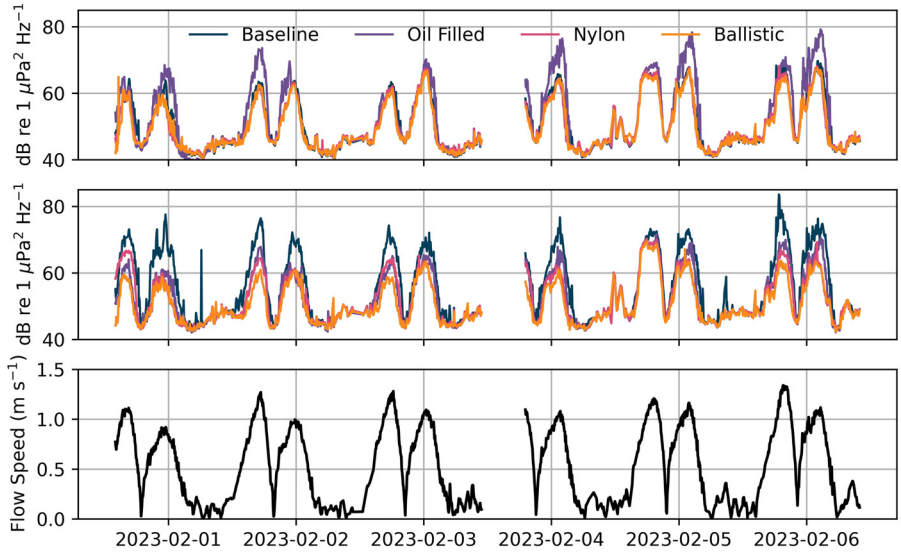

Fig. 5. Five-min average sound levels measured by each hydrophone at 927 Hz (top) and 2030 Hz (second from top) as a function of time. Flow speed is shown for context.

This hypothesis is supported by the fact that these signals vary between tidal cycles as kelp was entrained and pushed off of the lander by the tides, as well as by diver observations of kelp on the lander during recovery.

4. Discussion and conclusions

Of the three flow shields tested, the oil-filled shield most significantly reduced flow noise contamination at all frequencies, although flow noise contamination using the ballistic nylon shield was within 3 dB of contamination using the oil-filled shield above 80 Hz. No attenuation of propagating sound was associated with any of the shields, although further investigation of performance at higher frequencies is warranted. In addition to reducing flow noise contamination, the fabric shields may better protect from noise due to debris caught on the hydrophone element. While the thin nylon flow shield did not perform as well as the other two shields, it did reduce flow noise contamination and may still be a prudent solution in some scenarios given that it is significantly less complex to fabricate, more easily available, and cost effective. However, it may be more prone to biofouling than the other two shields tested; after our six-day deployment, organic material was caught in the thin nylon material. While this did not degrade hydrophone performance over this short test, the thin material acted like a net and may be more prone to biofouling over longer deployments than the other two designs. Further, as evidenced in Haxel and Henkel,[8] the thin nylon material is generally less robust and more likely to tear or come loose and produce unwanted noise.

Flow shields may improve low-frequency data quality for a variety of passive acoustic monitoring scenarios. Flow noise has been identified as a particularly relevant challenge for monitoring the sound produced by tidal or riverine energy converters due to their location at sites where flow speeds exceeding 1 m s^{-1} are typical.[20] Flow noise can also contaminate measurements at coastal sites where near-bottom wave orbital velocities can exceed 0.5 m s^{-1},[21] although turbulence characteristics are likely to be significantly different from those observed in a tidal channel. Hydrophone measurements from moving platforms, such as gliders, are also affected by flow noise[22] and may be candidates for flow shield application.

Several factors should be considered when applying the results presented in this work to other sites and hydrophone deployment configurations. First, while not the intent of the design, the design of the fabric shields protected the hydrophones from contact with drifting debris, which may be advantageous at sites where debris in the water column is expected. Second, the size and shape of the oil-filled shield directly affect its performance, while the form factors of the fabric flow shields are likely less significant. This is important to consider when adapting the oil-filled design for other hydrophones, because performance will likely differ from that reported here. While the semi-empirical model developed by Bassett *et al.*[4] can be applied to describe the relationship between turbulence and flow noise, it requires empirical tuning for the specific geometry (see supplemental Appendix). Future efforts to model the influence of hydrophone geometry on flow noise could facilitate optimized flow shield design. Additionally, even at the same current speeds, flow noise and flow shield performance will differ between sites due to differences in turbulence characteristics. Finally, in tidal channels, performance may differ between ebb and flood tides due to tidal asymmetry; this was observed in this test and is representative of other tidal channels.[23–25]

Supplementary material

See the supplementary material for supplemental figures and appendix.

Acknowledgments

The authors gratefully acknowledge the contributions of A. Barker, E. Walters, C. Rumple, C. Bassett, G. Staines, the Pacific Northwest National Laboratory dive team, and X-Flow Energy to this work. This work was funded by the United States Department of Energy, Water Power Technology Office under Contract No. DE-AC05-76RL01830.

Author Declarations

Conflict of Interest

The authors have no conflicts of interest to disclose.

Data Availability

The data that support the findings of this study are available from the corresponding author upon reasonable request.

References

[1]G. M. Wenz, "Acoustic ambient noise in the ocean: Spectra and sources," J. Acoust. Soc. Am. **34**(12), 1936–1956 (1962).
[2]R. Urick, *Principles of Underwater Sound* (Peninsula, Los Altos, CA, 1967), Chap. 11.
[3]M. Strasberg, "Nonacoustic noise interference in measurements of infrasonic ambient noise," J. Acoust. Soc. Am. **66**(5), 1487–1493 (1979).
[4]C. Bassett, J. Thomson, P. H. Dahl, and B. Polagye, "Flow-noise and turbulence in two tidal channels," J. Acoust. Soc. Am. **135**(4), 1764–1774 (2014).
[5]S. P. Robinson, P. A. Lepper, and R. A. Hazelwood, "Good practice guide for underwater noise measurement" (National Measurement Office, Teddington, UK, 2014).

[6]B. Wilson, P. A. Lepper, C. Carter, and S. P. Robinson, "Rethinking underwater sound-recording methods to work at tidal-stream and wave-energy sites," in *Marine Renewable Energy and Environmental Interactions, Humanity and the Sea*, edited by M. A. Shields and A. I. L. Payne (Springer, Dordrecht, Netherlands, 2014), pp. 111–126.
[7]S. B. Martin and A. N. Popper, "Short- and long-term monitoring of underwater sound levels in the Hudson River (New York, USA)," J. Acoust. Soc. Am. **139**(4), 1886–1897 (2016).
[8]J. H. Haxel and S. K. Henkel, "Measuring changes in ambient noise levels from the installation and operation of a surge wave energy converter in the coastal ocean," Report No. DOE-OSUHMSC-0006387 (USDOE Office of Energy Efficiency and Renewable Energy, Washington, DC, 2017).
[9]K. Raghukumar, G. Chang, F. Spada, and C. Jones, "A vector sensor-based acoustic characterization system for marine renewable energy," J. Mar. Sci. Eng. **8**(3), 187 (2020).
[10]C. Bassett, "Ambient noise in an urbanized tidal channel," Ph.D. thesis, University of Washington, Seattle, WA (2013).
[11]P. Porskamp, J. Broome, B. Sanderson, and A. Redden, "Assessing the performance of passive acoustic monitoring technologies for porpoise detection in a high flow tidal energy test site," Can. Acoust. **43**(3), 2768 (2015).
[12]S. Harding, K. Hall, J. Vavrinec, G. Harker-Klimes, and M. Richmond, "Field characterization of Triton tidal site: Vessel-mounted ADCP survey of Sequim Bay inlet," Report No. PNNL-25284 (Pacific Northwest National Laboratory, Richland, WA, 2016).
[13]S. Liang, B. Lashkari, S. S. S. Choi, V. Ntziachristos, and A. Mandelis, "The application of frequency-domain photoacoustics to temperature-dependent measurements of the Grüneisen parameter in lipids," Photoacoustics **11**, 56–64 (2018).
[14]W. Maurice, "Development of castor-oil-resistant urethane sonar encapsulants," Report No. ADA126415 (Naval Research Laboratory, Washington, DC, 1985).
[15]Naval Sea Systems Command, "Type H52 hydrophone," https://www.navsea.navy.mil/Portals/103/Documents/NUWC_Newport/USRD/H52.pdf (Last viewed November 16, 2023).
[16]J. A. Hildebrand, K. E. Frasier, S. Baumann-Pickering, and S. M. Wiggins, "An empirical model for wind-generated ocean noise," J. Acoust. Soc. Am. **149**(6), 4516–4533 (2021).
[17]L. Kilcher, "DOLfYN version 1.2.1," https://github.com/lkilcher/dolfyn (Last viewed October 1, 2023).
[18]T. L. Wahl, "Discussion of 'Despiking acoustic Doppler velocimeter data' by Derek G. Goring and Vladimir I. Nikora," J. Hydraul. Eng. **129**(6), 484–487 (2003).
[19]D. G. Goring and V. I. Nikora, "Despiking acoustic Doppler velocimeter data," J. Hydraul. Eng. **128**(1), 117–126 (2002).
[20]B. Polagye and C. Bassett, "Risk to marine animals from underwater noise generated by marine renewable energy devices," in *OES-Environmental 2020 State of the Science Report: Environmental Effects of Marine Renewable Energy Development around the World*, edited by A. E. Copping and L. G. Hemery (U.S. Department of Energy Office of Scientific and Technical Information, Washington, DC, 2020), pp. 67–85.
[21]P. L. Wiberg and C. R. Sherwood, "Calculating wave-generated bottom orbital velocities from surface-wave parameters," Comput. Geosci. **34**(10), 1243–1262 (2008).
[22]S. Fregosi, D. V. Harris, H. Matsumoto, D. K. Mellinger, S. W. Martin, B. Matsuyama, J. Barlow, and H. Klinck, "Detection probability and density estimation of fin whales by a Seaglider," J. Acoust. Soc. Am. **152**(4), 2277–2291 (2022).
[23]R. M. Horwitz and A. E. Hay, "Turbulence dissipation rates from horizontal velocity profiles at mid-depth in fast tidal flows," Renew. Energy **114**, 283–296 (2017).
[24]J. M. McMillan and A. E. Hay, "Spectral and structure function estimates of turbulence dissipation rates in a high-flow tidal channel using broadband ADCPs," J. Atmos. Ocean. Technol. **34**(1), 5–20 (2017).
[25]M. Thiébaut, N. Quillien, A. Maison, H. Gaborieau, N. Ruiz, S. MacKenzie, G. Connor, and J.-F. Filipot, "Investigating the flow dynamics and turbulence at a tidal-stream energy site in a highly energetic estuary," Renew. Energy **195**, 252–262 (2022).